Proceedings of the ASME Turbo Expo 2020: Turbomachinery Technical Conference and Exposition
GT2020
June 22-June 26, 2020, London, UK

GT2020-15943

DRAFT: A 3D TURBOMACHINERY DESIGN SYSTEM INTEGRATING PHYSICS-BASED PARAMETERIZATION WITH THE ENGINEERING SKETCH PAD

Mayank Sharma*
Gas Turbine Simulation Laboratory
Department of Aerospace Engineering
University of Cincinnati
Cincinnati, Ohio 45221
Email: sharmamm@mail.uc.edu

John F. Dannenhoffer, III
Department of Mechanical and Aerospace Engineering
Syracuse University
Syracuse, New York 13244
Email: jfdannen@syr.edu

Justin Holder
Mark G. Turner
Gas Turbine Simulation Laboratory
Department of Aerospace Engineering
University of Cincinnati
Cincinnati, Ohio, 45221
Email: holderjn@mail.uc.edu
turnermr@mail.uc.edu

ABSTRACT

This paper describes a turbomachinery blade generation system which integrates easily in an MDAO driven design process while providing the designer with a flexible and parsimonious parameterization scheme along with insights gained from interaction with 3D geometry. T-Blade3 *is an open source 3D parametric blade geometry generator which uses a novel parameterization scheme based on the specification of the second derivative of the mean-line and a continuous modified NACA four digit thickness distribution as B-spline control points. The second derivative parameterization ensures curvature and slope of curvature continuity on the airfoil surface which leads to a smooth surface pressure distribution. Use of spanwise B-spline control points ensures the creation of smooth 3D geometries and keeps the overall parameterization space small. The Engineering Sketch Pad (*ESP*) is an open-source interactive web-enabled solid modeling system based on* WebViewer *and* OpenCSM*. The open-source nature of* OpenCSM *allows the use of user-defined primitives to create solid blade models using* T-Blade3 *geometries.* OpenCSM *also allows the computation of the sensitivity of surface points to design parameters using a combination of analytical derivatives and finite differences. Thus, the* T-Blade3/ESP *combinations allows a designer to interact with parametrically generated geometries and make improvements to the design using sensitivity information and a gradient based optimization loop. Furthermore,* ESP *enables the addition of flends (similar to fillets) to solid blade models. The resulting blades with applied centrifugal and pressure loads are then analyzed with a commercial FEM structural solver to get factor of safety relative to yield strength, natural frequencies and mode shapes.*

NOMENCLATURE

a_i	Continuous modified NACA thickness distribution coefficients for $u < u_{\max}$
Cam	Total camber for blade section
chrd	Non-dimensional chord
chrd_mult	Chord multiplier
d_i	Continuous modified NACA thickness distribution coefficients for $u \geq u_{\max}$
f_s	Factor of safety
I	Leading edge radius parameter for continuous modified NACA thickness distribution
i	Incidence
k	Camber-line second derivative scaling factor
m'	Meridional coordinate
n_{blades}	Number of blades in bladerow

*Address all correspondence to this author.

n_{cp} Number of chordwise camber-line second derivative cubic B-spline control points
n_p Number of points along blade section surface
n_{span} Number of spanwise sections
$n_{\text{span,cm}}$ Number of spanwise chord multiplier B-spline control points
$n_{\text{span,sweep}}$ Number of spanwise axial sweep B-spline control points
$n_{\text{span,curv}}$ Number of spanwise camber-line second derivative B-spline control points
$n_{\text{span,sweep}}$ Number of spanwise axial sweep B-spline control points
$n_{\text{span,LE}}$ Number of spanwise inlet angle modifier B-spline control points
$n_{\text{span,lean}}$ Number of spanwise tangential lean B-spline control points
$n_{\text{span,TE}}$ Number of spanwise exit angle modifier B-spline control points
$\bar{r}$ Non-dimensionalized span
$n_{\text{span,thk}}$ Number of spanwise thickness B-spline control points
r Radial coordinate
scf Dimensional blade scaling factor
u Non-dimensional chord-line coordinate
v Non-dimensional coordinate perpendicular to u
v_m Non-dimensional camber-line coordinate
v_t Non-dimensional thickness coordinate
x Axial coordinate

Greek Symbols

α Clustering parameter
β Flow angle
β^* Blade metal angle
δ Deviation
θ Tangential coordinate
ξ Stagger angle

Subscripts

b Blade section
bot Blade section bottom surface
LE Leading edge
lean Spanwise tangential lean definition
s Streamline
stack Stacking location in (u, v) space
sweep Spanwise axial sweep defintion
TE Trailing edge
top Blade section top surface

Abbreviations

2D Two dimensional
3D Three dimensional
BLI Boundary layer ingestion
DM ANSYS Design Modeler
CAD Computer Aided Design
ESP The Engineering Sketch Pad
GUI Graphical user interface
MDAO Multidisciplinary analysis and optimization
NURBS Non uniform rational B-spline
PCG Preconditioned Conjugate Gradient
UDP User defined primitive

INTRODUCTION

Turbomachinery aerodynamic shape optimization has seen a boost with the adoption of multidisciplinary analysis and optimization (MDAO) strategies enabled by advancements in numerical algorithms and computer hardware. As part of this process, a fast, parametric blade geometry generator based on an understanding of the flow properties of a turbomachinery blade is required.

Many previous efforts at developing parametric geometry generators can be found in the literature. Korikianitis [1] described a method of generating the blade section by using a prescribed surface curvature distribution for the blade surface while specifying the leading edge as a thickness distribution and using a polynomial based trailing edge shape. A general approach was presented by Kulfan [2] for the construction of round nose/sharp trailing edge airfoils. This resulted in the use of a well behaved analytic shape function for geometry generation combined with a class function for generalization. Gräsel et al. [3] discussed a non uniform rational B-spline (NURBS) based parametric geometry generator which can produce blades based either on the superposition of a mean-line and a thickness distribution or the direct specification of pressure and suction sides while ensuring curvature continuity. Dutta et al. [4] have described a geometry generator based on a Bezier curve representation of the camber-line slope. The blade generation is completed by adding a thickness distribution to the resulting camber-line. Bezier curves are also used to radially parameterize metal blade angles. Koini et al. [5] describe a parametric turbomachinery design tool, T4T, which constructs a camber-line based on a NURBS representation of it with three control points two of which are fixed at the leading and trailing edges. The suction and pressure sides of the blade section are constructed by placing points normal to the camber line.

Integration of a geometry generator with a computer aided design (CAD) package introduces interactivity in a design tool. BladeCAD [6] was an interactive design tool developed under NASA supervision and used a NURBS to create 2D blade sections using the superposition of a camber line with a non-symmetric thickness distribution. The 2D sections were stacked on surfaces of revolution to create a 3D blade. A more recent example is ANSYS BladeModeler [7] which is integrated with ANSYS DesignModeler to obtain 3D blades.

T-Blade3 (formerly 3DBGB [8, 9]) is an open source 3D parametric blade geometry generator which uses a parameterization scheme based on the second derivative of the camber-line, related to curvature, which is specified using cubic B-spline con-

trol points and integrated twice to obtain the mean-line. Turner [10] has discussed the intuitive changes made to blade loading by manipulating the curvature of the mean-line of a lightly loaded swirler-deswirler vane while Balasubramanian et al. [11] have discussed the importance of using B-splines to represent the second derivative of the camber-line in reducing curvature and slope-of-curvature continuities thus developing a smooth pressure distribution of the blade. To complete the blade section generation, a smooth thickness distribution is added symmetrically to both sides of the mean-line.

While a discussion of aerodynamic shape optimization is outside the scope of this paper, T-Blade3 has been used as the geometry generator for some MDAO processes. Mandal [12] has described the design and optimization of a three bladerow propulsor for boundary layer ingestion (BLI) using a Genetic Algorithm based optimizer from DAKOTA [13]. Another study of BLI fans using T-Blade3 was carried out by Sieradzki et al. [14]. Ugolotti et al. applied a discrete adjoint capability to the aerodynamic shape optimization of a turbine cascade and utilized design parameters originating from T-Blade3 as degrees of freedom of the optimization problem [15]. A similar study was carried out by Viars [16] where T-Blade3 design parameters and geometries were used in concert with the MISES [17] flow solver and a constrained gradient based optimization process driven by OpenMDAO [18] to minimize a loss coefficient while holding the exit flow angle constant.

This paper describes the geometry generation process in T-Blade3 and discusses its integration with the Engineering Sketch Pad (ESP) [19]. ESP is a parametric, feature based, web-enabled solid modeling system. It allows the creation of interactive solid blade models. This integration is explored further along in this paper.

The paper is structured as follows. First, the T-Blade3 geometry generation process is discussed. The discussion starts with an explanation of the coordinate systems and transformations involved in moving from an initial 2D blade section to a final stacked 3D blade. Construction of the mean-line is discussed next followed by the construction of the thickness distribution and generation of the initial 2D blade section. Spanwise variation of the design parameters is detailed next and a summary of the parameterization is presented. Next, the integration of T-Blade3 with ESP is discussed which includes a demonstration of the solid blade modeling capability of ESP and is rounded off with a demonstration of flends (filleted blends) in ESP. Finally, a structural analysis using ANSYS Workbench Mechanical with the solid blade geometry for a factor of safety computation is presented to illustrate an application of the design system.

Discussions of the design system in this paper use a single example case detailed by Mandal [12] (Case 7-28-5 rotor). This case was chosen to coherently show the design system in action but this paper is not a summary of this particular design.

GEOMETRY GENERATION

Coordinate Systems

The geometry creation process, discussed further below, begins in a chord normalized, zero stagger, non dimensional space (u,v) with $u \in [0,1]$. The chord line u is clustered towards $u=0$ and $u=1$ and is constructed using one of several clustering algorithms. The mean-line v is constructed using the second derivative of the mean-line. The thickness distribution v_t is also superimposed in the (u,v) space.

The stacked non-dimensional blade section (u_b, v_b) is defined as the combination of its bottom surface $(u_{b,\text{bot}}, v_{b,\text{bot}})$ and its top surface $(u_{b,\text{top}}, v_{b,\text{top}})$. These surfaces are obtained as:

$$\begin{aligned} u_{b,\text{bot}} &= u_{\text{bot}} - u_{\text{stack}} \\ v_{b,\text{bot}} &= v_{\text{bot}} - v_{\text{stack}} \\ u_{b,\text{top}} &= u_{\text{top}} - u_{\text{stack}} \\ v_{b,\text{top}} &= v_{\text{top}} - v_{\text{stack}} \end{aligned} \tag{1}$$

where $(u_{\text{stack}}, v_{\text{stack}})$ is the spanwise stacking location, which is a user-defined input. Equations 15 to 18 define the non-dimensional blade section surfaces $(u_{\text{bot}}, v_{\text{bot}})$ and $(u_{\text{top}}, v_{\text{top}})$.

Next, the (u_b, v_b) blade section is rotated by the stagger angle ξ and scaled by a non-dimensional chord *chrd* to yield a (m'_b, θ_b) section as:

$$\begin{aligned} m'_b &= chrd\,(u_b \cos(\xi) - v_b \sin(\xi)) \\ \theta_b &= chrd\,(u_b \sin(\xi) + v_b \cos(\xi)) \end{aligned} \tag{2}$$

Figure 1 shows the relation between the (u_b, v_b) and (m'_b, θ_b) blade sections.

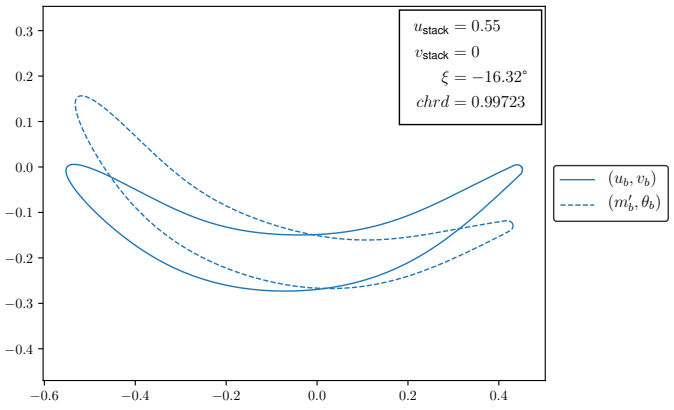

FIGURE 1: CASE7-28-5 ROTOR HUB SECTION IN (u_b, v_b) SPACE AND (m'_b, θ_b) SPACE.

The (m'_b, θ_b) sections are mapped on to their corresponding surfaces of revolution (axisymmetric streamlines). A cubic spline fit is used for the streamline coordinates (x_s, r_s), which originate from T-AXI [20], with m'_s as the spline parameter which is defined as:

$$m'_s = \int \frac{\sqrt{(dr_s)^2 + (dx_s)^2}}{r_s} \tag{3}$$

The leading edge value $m'_{s,\mathrm{LE}}$ is obtained by intersecting initial axisymmetric values of the leading and trailing edges of the blade, again originating from T-AXI, with the m'_s cubic spline. For precise mapping of the (m'_b, θ_b) sections on to the streamlines, a meridional offset is needed since the zero m'_s is different from the blade section leading edge $m'_{b,\mathrm{LE}}$. This offset is:

$$\delta m' = m'_{s,\mathrm{LE}} - m'_{b,\mathrm{LE}} \tag{4}$$

A modified spline parameter $m'_{b,s}$ is thus obtained. This spline parameter also includes the sweep definition $\delta m'_{\mathrm{sweep}}$, which is computed using spanwise B-splines. Thus:

$$m'_{b,s} = m'_b + \delta m' + \delta m'_{\mathrm{sweep}} \tag{5}$$

$m'_{b,s}$ is used in an inverse spline operation to obtain (x_b, r_b, θ_b) coordinates for the (m'_b, θ_b) geometry. Finally, the (x, y, z) coordinates are obtained as:

$$\begin{aligned} x &= scf * x_b \\ y &= scf * r_b \cos(\theta_b + \delta\theta_{\mathrm{lean}}) \\ z &= scf * r_b \sin(\theta_b + \delta\theta_{\mathrm{lean}}) \end{aligned} \tag{6}$$

where $\delta\theta_{\mathrm{lean}}$ is the spanwise lean definition and scf is a dimensional scaling factor. Figure 2 shows hub, midspan and tip (x, y, z) sections for the Case7-28-5 rotor.

Blade Section Generation

Mean-line Construction The chord-line u is constructed first with a user-defined number of points n_p. The chordline is clustered towards $u = 0$ and $u = 1$ to achieve clustering of points at the blade section leading edge and trailing edge. A simple clustering algorithm leads to:

$$\delta u_j = u_j - u_{j-1} = \sin^{\alpha}\left(\frac{\pi(j-1)}{n_p}\right) \tag{7}$$

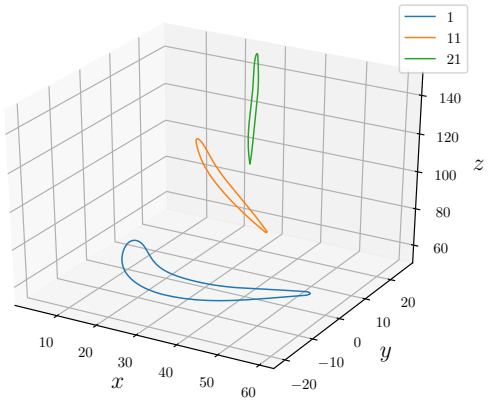

FIGURE 2: CASE 7-28-5 ROTOR (x, y, z) HUB SECTION (SECTION 1), MIDSPAN SECTION (SECTION 11) AND TIP SECTION (SECTION 21).

where $2 \leq j \leq n_p$ is an index with $u_1 = 0.0$ and $u_{n_p} = 1.0$ and α is a user-defined clustering parameter. A higher value of α leads to greater clustering at the leading and trailing edges.

Several camber-line definitions are available in T-Blade3 including a cubic camber-line and a mixed camber-line. The preferred method for camber-line construction has been detailed by Balasubramanian et al. [11], with some equations therein reproduced here, and involves reading in the control points of the second derivative of the camber-line $v''_m(u)$ as control points for a cubic B-spline. The camber-line $v_m(u)$ is thus obtained as:

$$v'_m(u) = k \int v''_m(u)du + C_1 \tag{8}$$

$$v_m(u) = k \iint v''_m(u)du + C_1 u + C_2 \tag{9}$$

where C_1 and C_2 are constants of integration and k is a scaling factor for the B-spline control points. k, C_1 and C_2 are computed by employing the following boundary conditions:

$$v_m(0) = 0 \tag{10}$$

$$v_m(1) = 0 \tag{11}$$

$$\tan^{-1}(v'_m(1)) - \tan^{-1}(v'_m(0)) = Cam = \beta^*_{\mathrm{LE}} - \beta^*_{\mathrm{TE}} \tag{12}$$

where Cam is the total camber of the blade, β^*_{LE} is the inlet blade metal angle and β^*_{TE} is the exit blade metal angle. This leads to a completely analytical definition of the camber-line. Figure 3 shows the camber-line second derivative cubic B-spline control points along with the B-splines for the hub, midspan and tip

sections of Case7-28-5 and Figure 4 shows the corresponding computed camber-line definitions. The plot shows that the second derivative can change sign. This implies an inflection point in the meanline itself.

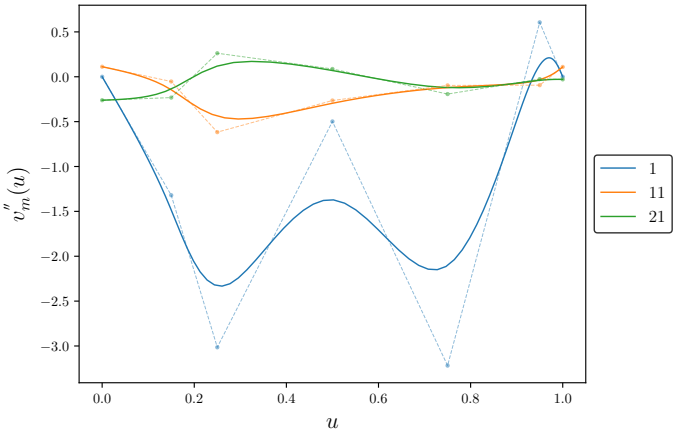

FIGURE 3: CAMBER-LINE SECOND DERIVATIVE AND SCALED CONTROL POINTS FOR CASE 7-28-5 HUB SECTION (SECTION 1), MIDSPAN SECTION (SECTION 11) AND TIP SECTION (SECTION 21).

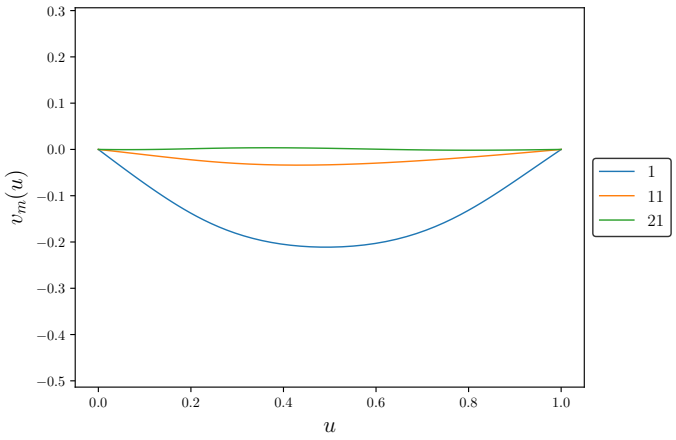

FIGURE 4: CAMBER-LINE DEFINITIONS FOR CASE 7-28-5 HUB SECTION (SECTION 1), MIDSPAN SECTION (SECTION 11) AND TIP SECTION (SECTION 21).

Thickness Distribution There are several thickness distribution options available in T-Blade3 including a Wennerstrom thickness distribution [21,8] and a quartic spline thickness distribution [9]. Case 7-28-5 uses a continuous modified NACA four digit thickness distribution [22,23] which is defined as:

$$v_t(u) = a_0\sqrt{u} + a_1 u + a_2 u^2 + a_3 u^3 \qquad \text{for } 0 \le u < u_{\max} \tag{13}$$

$$v_t(u) = d_0 + d_1(1-u) + d_2(1-u)^2 + d_3(1-u)^3 \text{ for } u_{\max} \le u \le u_{\mathrm{TE}} \tag{14}$$

with C2 continuity at $u_{\max}$, where $u_{\max}$ is the chordwise location of the maximum thickness and $u_{\mathrm{TE}} \le 1$ is the location of the trailing edge. The trailing edge can either be sharp ($u_{\mathrm{TE}} = 1$) or circular ($u_{\mathrm{TE}} < 1$). This distribution allows control over the leading edge radius of curvature unlike the standard NACA four digit definition. Figure 5 shows the thickness distribution for the hub, midspan and tip sections of the Case 7-28-5 rotor.

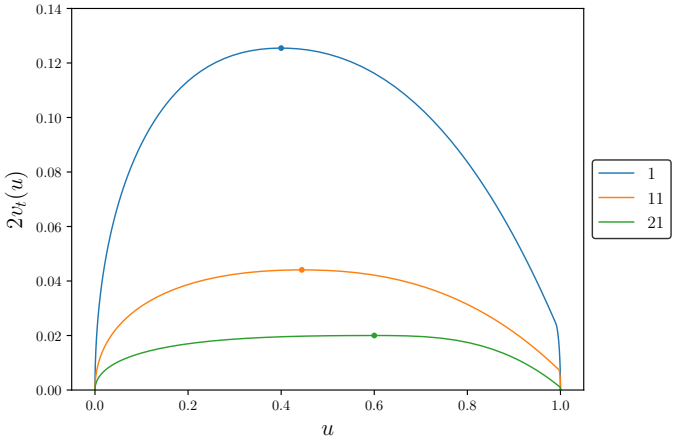

FIGURE 5: THICKNESS DISTRIBUTIONS AND MAXIMUM THICKNESS LOCATIONS FOR CASE 7-28-5 HUB SECTION (SECTION 1), MIDSPAN SECTION (SECTION 11) AND TIP SECTION (SECTION 21).

Non-Dimensional Blade Section Once, the camber-line and thickness distribution has been constructed, the top and bottom surfaces of the non-dimensional blade section are obtained as:

$$u_{\mathrm{bot}} = u \quad + v_t \sin(\tan^{-1}(v_m')) \tag{15}$$

$$v_{\mathrm{bot}} = v_m - v_t \cos(\tan^{-1}(v_m')) \tag{16}$$

$$u_{\mathrm{top}} = u \quad - v_t \sin(\tan^{-1}(v_m')) \tag{17}$$

$$v_{\mathrm{top}} = v_m + v_t \cos(\tan^{-1}(v_m')) \tag{18}$$

Figure 6 shows non-dimensional hub, midpsan and tip sections for the Case 7-28-5 rotor.

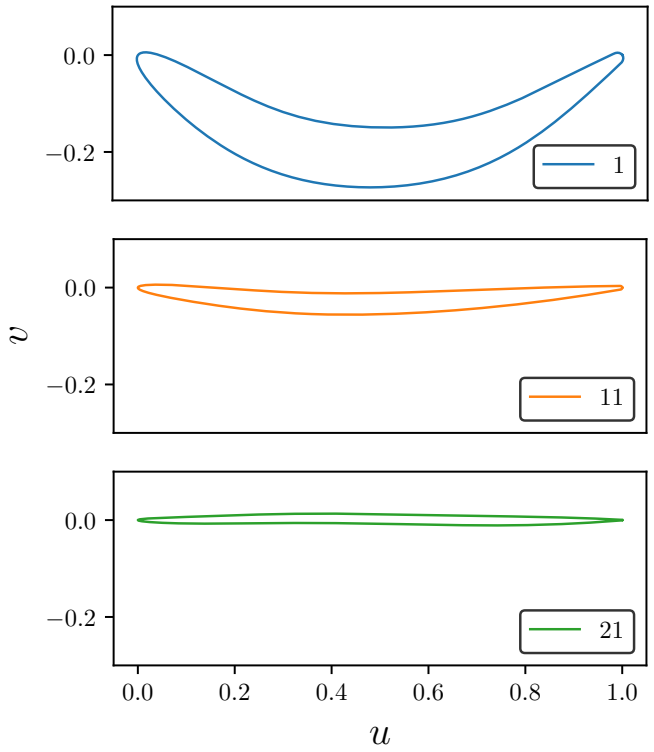

FIGURE 6: CASE 7-28-5 ROTOR (u,v) HUB SECTION (SECTION 1), MIDSPAN SECTION (SECTION 11) AND TIP SECTION (SECTION 21).

Spanwise Variation

T-Blade3 uses cubic B-splines for smooth spanwise variation of various parameters as described by Mahmood et al. [24]. Thus, as an example, the second derivative of the camber-line is represented by both chordwise and spanwise cubic B-spline control points where the total number of control points is user-defined. Similarly, the axial sweep $\delta m'_{\text{sweep}}$ (Equation 5 is for the axial sweep) and the tangential/true lean $\delta\theta_{\text{lean}}$ (Equation 6 is for the tangential lean) definitions, if present, are constructed using spanwise B-splines. A final instance is the use of these spanwise B-splines to define modifications to the leading and trailing edge angles, $\Delta\beta_{\text{LE}}$ and $\Delta\beta_{\text{TE}}$ respectively, for all sections which are combined with the flow angles $(\beta_{\text{LE}}, \beta_{\text{TE}})$ to compute blade metal angles $(\beta^*_{\text{LE}}, \beta^*_{\text{TE}})$ in accordance with the following relations:

$$\Delta\beta_{\text{LE}} = \begin{cases} \beta_{\text{LE}} - \beta^*_{\text{LE}} & \text{if } \beta^*_{\text{LE}} > 0 \\ \beta^*_{\text{LE}} - \beta_{\text{LE}} & \text{if } \beta^*_{\text{LE}} < 0 \end{cases} \tag{19}$$

$$\Delta\beta_{\text{TE}} = \begin{cases} \beta_{\text{TE}} - \beta^*_{\text{TE}} & \text{if } Cam < 0 \\ \beta^*_{\text{TE}} - \beta_{\text{TE}} & \text{if } Cam > 0 \end{cases} \tag{20}$$

The spanwise B-spline fits use a non-dimensionalized span defined as:

$$\bar{r} = \frac{r_{\text{LE},i_{\text{span}}} - r_{\text{LE},1}}{r_{\text{LE},n_{\text{span}}} - r_{\text{LE},1}} \tag{21}$$

where $1 \leq i_{\text{span}} \leq n_{\text{span}}$ is an index for spanwise blade sections with $i_{\text{span}} = 1$ denoting the hub section and $i_{\text{span}} = n_{\text{span}}$ denoting the tip section. Figure 7 shows the spanwise definition of $v''_m(u)$ at $u = 0.5$ while Figure 8 shows the spanwise variation of $\Delta\beta_{\text{LE}}$ and $\Delta\beta_{\text{TE}}$ for the Case 7-28-5 rotor.

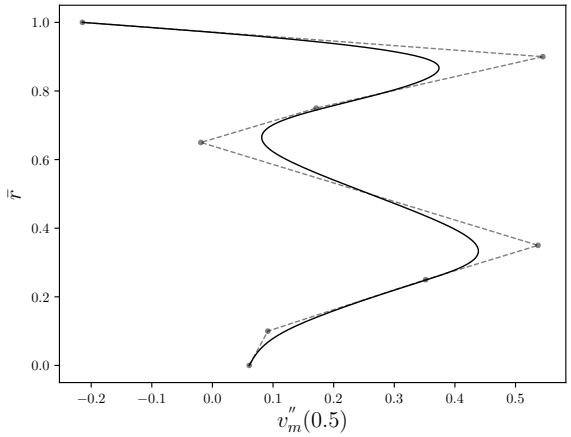

FIGURE 7: SPANWISE DEFINITION OF SECOND DERIVATIVE OF CAMBER LINE AT MIDCHORD FOR CASE 7-28-5 ROTOR ALONG WITH B-SPLINE CONTROL POINTS.

On Parameterization

The parameterization in T-Blade3, for most cases, is summarized in Table 1.

It should be noted that the number of the various spanwise B-spline control points need not equal each other or the number of spanwise sections n_{span}. The number of inputs for the parameters $v''_m(u)$, $v_t(u)$, $\delta m'_{\text{sweep}}$, $\delta\theta_{\text{lean}}$, $\Delta\beta_{\text{LE}}$, $\Delta\beta_{\text{TE}}$ and

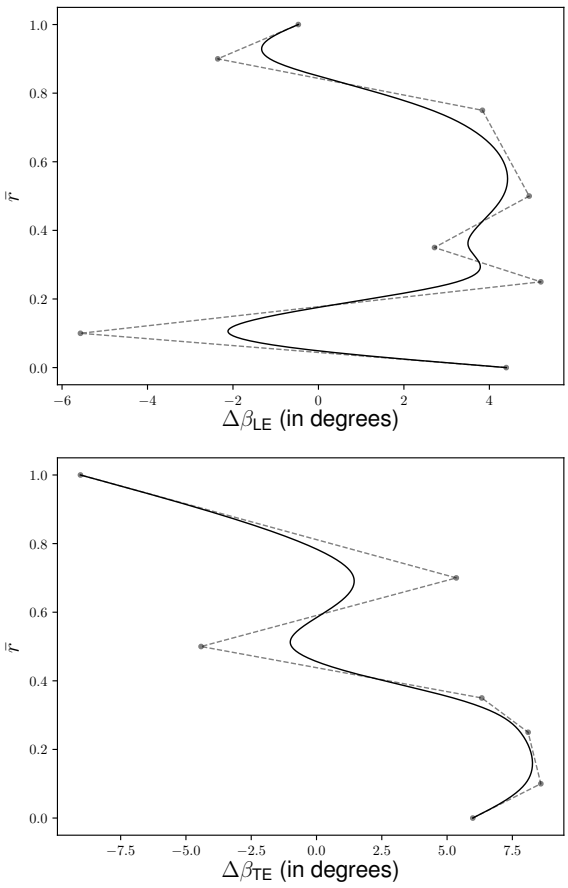

FIGURE 8: SPANWISE DEFINITIONS OF LEADING AND TRAILING EDGE ANGLE MODIFICATIONS FOR CASE 7-28-5 ROTOR ALONG WITH B-SPLINE CONTROL POINTS.

chrd_mult include the number of spanwise control points for the non-dimensional span $\bar{r}$. Thus, the spanwise axial sweep is defined through $n_{\text{span,sweep}}$ control points $(\bar{r}, \delta m'_{\text{sweep}})$. For the hub section $\bar{r} = 0$ and for the tip section $\bar{r} = 1$ which leads to the total number of inputs becoming $2n_{\text{span,sweep}} - 2$. In the case of the camber-line second derivative $v''_m(u)$, there are n_{cp} chordwise B-spline control points $(u, v''_m(u))$ but the values of u at the leading edge and trailing edge are fixed as $u = 0$ and $u = 1$ respectively which leads to the number of inputs for the camber-line second derivative sectionwise splines as $2n_{cp} - 2$. Now, each section also has a spanwise B-spline control point for $\bar{r}$ attached to it leading to the total number of sectionwise inputs for $v''_m(u)$ as $2n_{cp} - 1$. Finally, this quantity is multiplied by the number of spanwise control points $n_{\text{span,curv}}$, again accounting for the fixed values of $\bar{r}$ for the hub and tip sections, which gives the total number of inputs as $(2n_{cp} - 1)(n_{\text{span,curv}}) - 2$. The number of inputs for all other parameters can be computed in a similar manner.

For a typical design and shape optimization instance, the following is typical:

$$
\begin{aligned}
n_{cp} &= 7 \\
n_{\text{span,curv}} &= 5 \\
n_{\text{span,thk}} &= 5 \\
n_{\text{span,sweep}} &= 5 \\
n_{\text{span,lean}} &= 5 \\
n_{\text{span,LE}} &= 5 \\
n_{\text{span,TE}} &= 5 \\
n_{\text{span,cm}} &= 5
\end{aligned}
$$

which leads to 133 inputs which can be varied in an optimization for a single blade row. This has been too many for a Genetic Algorithm driven optimization so, to get around this problem, often in the sectionwise camber-line second derivative B-spline control points, the u values stay fixed or the different parameters get optimized in subsequent optimization runs. This process has worked so far because the parameters are nearly orthogonal to each other and have a limited spanwise and chordwise extent because they are based on B-splines. Future optimization approaches based on the adjoint method and gradient based optimization will attempt to open up the entire design space at once.

Parameter	Total Number of Inputs	Open to ESP
n_{blades}	1	No
u_{stack}	1	No
v_{stack}	1	No
$v''_m(u)$	$(2n_{cp} - 1)(n_{\text{span,curv}}) - 2$	Yes
$v_t(u)$	$6n_{\text{span,thk}} - 2$	Yes
β_{LE}	n_{span}	No
β_{TE}	n_{span}	No
chrd	n_{span}	No
$\delta m'_{\text{sweep}}$	$2n_{\text{span,sweep}} - 2$	Yes
$\delta\theta_{\text{lean}}$	$2n_{\text{span,lean}} - 2$	Yes
$\Delta\beta_{LE}$	$2n_{\text{span,LE}} - 2$	Yes
$\Delta\beta_{TE}$	$2n_{\text{span,TE}} - 2$	Yes
chrd_mult	$2n_{\text{span,cm}} - 2$	Yes

TABLE 1: T-Blade3 PARAMETERIZATION SCHEME.

INTEGRATION WITH ESP

Overview of ESP

mCAD systems, which include many commercial CAD packages such as SolidWorks, CATIA or Pro/ENGINEER, operate on the principle of modifying or morphing an initial, often simple, shape to generate the final shape in a way that mimics manufacturing processes [25]. The models obtained from these systems are often not parameterically driven. aCAD systems, on the other hand, are parametric systems which generate models which can be simultaneously analyzed for their performance in a given setting. A familiar and flexible parameterization allows attainment of the design goal while improving understanding of automated optimization processes [26].

The Engineering Sketch Pad (ESP) is an aCAD system geared towards design and analysis of aerospace vehicles. While ESP itself can be used for development of solid models, it has been embedded in other design and analysis systems [27, 28, 29] or grid generation systems [30]. While a design feedback loop between aCAD and mCAD systems is not possible, due to differences in the solid modeling techniques, ESP can communicate with a mCAD system through the use of .step files, as shown in the structural analysis section. ESP is built upon the OpenCSM constructive solid modeler [31], which is built upon the Engineering Geometry Aircraft Design System (EGADS) [32], which in turn is built upon OpenCASCADE [33].

The T-Blade3/ESP System

ESP master models are defined using a Feature Tree and a set of design parameters, both of which are explained in detail by Dannenhoffer and Haimes [26].

The Feature Tree is a binary tree which contains a set of instructions detaling the operations needed to build the current configuration. Thus, as an example, the Feature Tree for building the configuration shown in Figure 10b consists of loading the two primitives (the blade and the hub surface of revolution, the *hubwedge*), which themselves are defined in their respective user defined primitives (UDPs) discussed further below, followed by a boolean Union operation.

As mentioned in the next section, the UDPs that generate the blade and hubwedge primitives execute T-Blade3 to do so. This involves building ESP from source and then compiling T-Blade3 from source (using a modified Makefile) to make a T-Blade3 library and object files available to ESP. This process informs much of the following discussion.

For the T-Blade3/ESP system, the design parameters are derived from the parameterization in T-Blade3 detailed in Table 1. Some parameters are not open to ESP, which means that their initial values set in T-Blade3 input files cannot be altered by ESP during a run of the T-Blade3/ESP system. Depending on the desired configuration, any number of the parameters open to ESP can be overridden. This imparts flexibility to the system while also providing a quick way for the designer to view the geometry created with T-Blade3 using ESP's graphical user interface (GUI) by not overriding any parameters. Since this process is automated there is no need to manually build a solid geometry using a mCAD system. An example of this is shown in Figure 10a. The integration of T-Blade3 with ESP has also proven useful in defining a design parameter space with all optimizations using this system only working with the parameters open to ESP.

Both the Feature Tree and design parameters for a given configuration are derived from and defined in ESP's input file which is an ASCII file with the extension .csm. Any active design parameters in this file are overridden by ESP during a run of the present system. The design parameters can be further modified using ESP's GUI after a successful run which doesn't require using the .csm file again. Furthermore, sensitivities of the model to any design parameters [34] can also be computed using the GUI. Any operations on the primitives (e.g. Union) are also outlined in the .csm file. These input files, in addition to T-Blade3's input files, are available for various cases on https://github.com/GTSL-UC/T-Blade3.git.

In addition to acting as a solid model generator and visualizer for T-Blade3 geometries, which also includes the option to export the finished geometry to a mCAD system if required, the T-Blade3/ESP system also lends itself to the development of automated design processes as described by Holder et al. [35]. The analytic sensitivity computation capabilities of ESP are also being leveraged for the development of a gradient based optimization process geared towards turbomachinery which is currently in consideration.

User Defined Primitives for T-Blade3/ESP

ESP is extensible through user defined primitives. The standard primitives in ESP include shapes like a box, sphere, cone or cylinder and more. Creation of complex configurations often requires the use of UDPs when standard primitives are not applicable. These UDPs create one primitive solid using standard formulations (e.g. NACA 4-digit airfoil) or through the use of several EGADS operations which can be analogous to certain mCAD operations (e.g. skinning/lofting). The creation of a turbomachinery blade and corresponding surfaces of revolution using T-Blade3 outputs is outlined below. The corresponding UDPs are included with the T-Blade3 source code instead of ESP.

The UDPs that integrate T-Blade3 with ESP perform the following operations:

1. the user supplies the name of standard T-Blade3 input files as well as values that can override some or all of the initial design parameter values
2. T-Blade3 is executed
3. the hub and tip output files are read to generate surfaces of revolution that will act at the ends of the blade

4. several (typically 21) input section files are read and B-spline approximations are created. This is done with a least-squares optimizer that varies the control point locations so as to minimize the rms distance of the points read from the section files from the resulting B-spline. An example of this fit is shown in Figure 9, where the whole hub section is shown in part (a), the leading edge region in part (b), and the trailing edge region in part (c). In each case, the circles represent the points read from T-Blade3, the squares are the control point locations, the dashed lines represent the control polygon, and the solid line the B-spline. For each section, there is a fixed number of evenly-spaced knots. This is done to reduce the number of points along the blade surface compared to the initial T-Blade3 geometry.
5. the B-spline curves created above form the bases of a tensor-product B-spline surface through a standard "skinning" operation. Since the B-spline curves all have the same knot sequence, the skinning operation does not introduce any further approximations.
6. the blades are capped with portion of the surfaces of revolution that were created in the first step

The resulting geometries, including a solid model of the blade and a Union of the solid blade and a hubwedge, are shown in Figure 10. The unusual spanwise variation of corresponding leading edge and trailing edge angle modifiers, $\Delta\beta_{\mathrm{LE}}$ and $\Delta\beta_{\mathrm{TE}}$ respectively (see Figure 8), was chosen to accomplish large spanwise distortions for boundary layer ingestion as detailed in [12]. This results in the "waviness" exhibited by the final blade.

Flends

A flend [36] is a B-spline surface that has some characteristics of a fillet and some of a blend (and hence the name flend). The flends are created so as to be tangent (C1) to the adjoining surface and nearly curvature continuous (C2); this is in contrast to fillets, which are, by definition, only C1, with large curvature discontinuities. These discontinuities that are associated with fillets are troublesome aerodynamically. Figures 11 and 12 show a flend generated for the Case 7-28-5 rotor.

INTEGRATION WITH STRUCTURAL ANALYSIS

The structural analysis of the Case 7-28-5 rotor with applied centrifugal and pressure loads for factor of safety computation is presented in this section. This analysis is meant to serve as an application of the T-Blade3/ESP system along with an automated and iterative hot-to-cold transformation process for turbomachinery, detailed by Holder et al. [35]. To facilitate this, an existing UDP has been modified to read (x,y,z) sections from which deformations computed by ANSYS Workbench Mechanical are subtracted to yield the cold shape, which is then modeled using ESP to get the new blade shape.

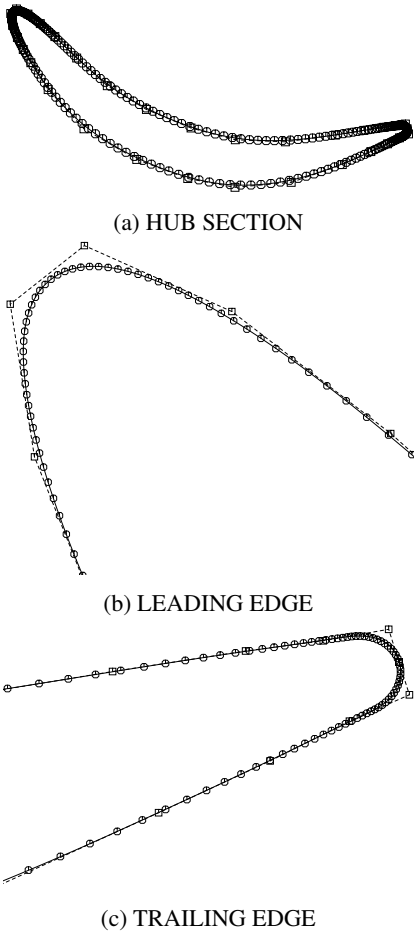

(a) HUB SECTION

(b) LEADING EDGE

(c) TRAILING EDGE

FIGURE 9: B-SPLINE APPROXIMATION OF HUB SECTION CREATED BY ESP.

Orthogonality of the thickness to the camber-line and lean definitions along with smooth spanwise variation of the parameters make the T-Blade3 parameterization well suited to design with respect to structural concerns.

The design process of the Case 7-28-5 rotor begins with the design of a geometry based on an operating point specification. This initial design is then optimized for aerodynamic efficieny, as described in [12]. At this stage the optimization is uncoupled from structural concerns. The flow optimized blade is checked for structural integrity using T-Blade3/ESP to generate the solid model shown in Figure 10b and then analyzed using the finite element solver, ANSYS Workbench Mechanical, for a factor of safety requirement. The design is altered through the use of certain T-Blade3 parameters. For the present case, these were mainly the maximum thickness $v_t(u_{\max})$, the trailing edge thickness $v_t(u_{\mathrm{TE}})$, the spanwise lean and sweep definitions, $\delta m'_{\mathrm{sweep}}$ and $\delta\theta_{\mathrm{lean}}$ respectively along with the chord multiplier, *chrd_mult*.

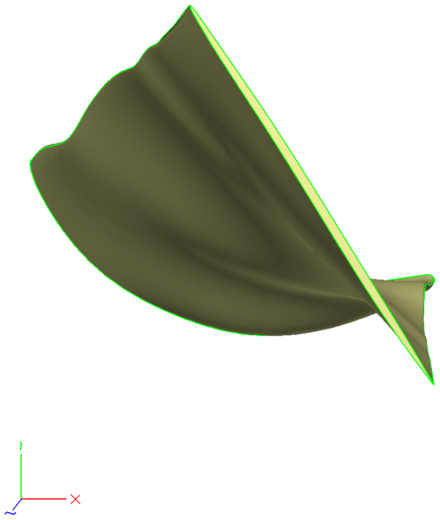

(a) BLADE MODEL

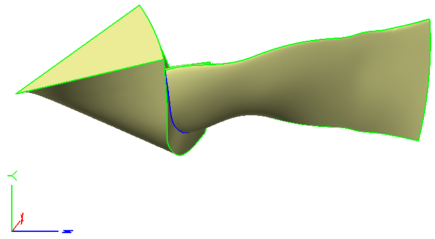

(b) INTERSECTION OF BLADE WITH HUBWEDGE

FIGURE 10: DEMONSTRATION OF GEOMETRIES CREATED BY INTEGRATION OF T-Blade3/ESP.

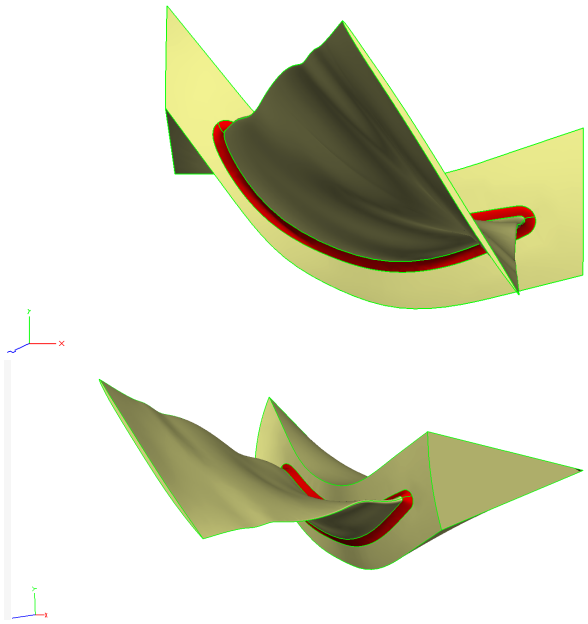

FIGURE 11: DEMONSTRATION OF ESP FLENDS FOR CASE 7-28-5 ROTOR.

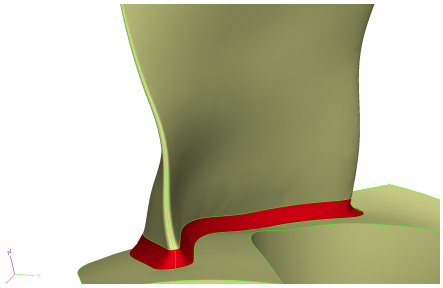

(a) TRAILING EDGE CLOSEUP

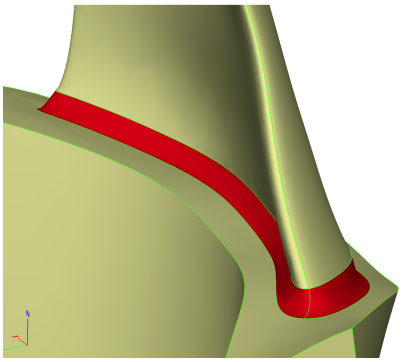

(b) LEADING EDGE CLOSEUP

FIGURE 12: CLOSEUPS OF FLENDS FOR CASE 7-28-5 ROTOR.

Finite Element Analysis

The cyclically symmetric *.step file output from ESP was first loaded into ANSYS DesignModeler (DM) in order to merge several tangent face pairs. The blade was assigned Ti-6Al-4V alloy [37]. A fillet was then added to the solid in DM. The mesh consisted of 10 node tetrahedrons (SOLID187) and 4 node surface (SURF154) elements where the latter was to account for the applied pressure loads. Further details of the mesh and grid density study can be found in [35]. Pressure data was extracted from NUMECA CFView following a steady mixing-plane analysis with FINE/Turbo.

The iterative Preconditioned Conjugate Gradient (PCG) solver was used with default convergence tolerance for the nonlinear Static Structural analysis. The structural solution was computed over five load steps where the rotation speed was ramped from 0 (step one), 50 (step two), 80 (step three), and 100% (steps four and five). Pressure loads were applied on the final load step. Modal analysis was performed for load steps one, two, three, and five using the iterative Lanczos PCG solver to extract *up to*

40 modes in the range 250 to 16000 Hz.

Figure 13 shows the contour of yield safety factor at design speed. Primary stress concentrations are located at approximately 30% span on the pressure side of the blade. There is also a lesser concentration near blade root at the trailing edge of the suction side. Both stressed areas are primarily due to the untwist and unlean of the blade under centrifugal loading. Despite the stress concentrations, Case 7-28-5 meets the structural integrity requirements of $f_s \geq 1.1$ at 110% design speed.

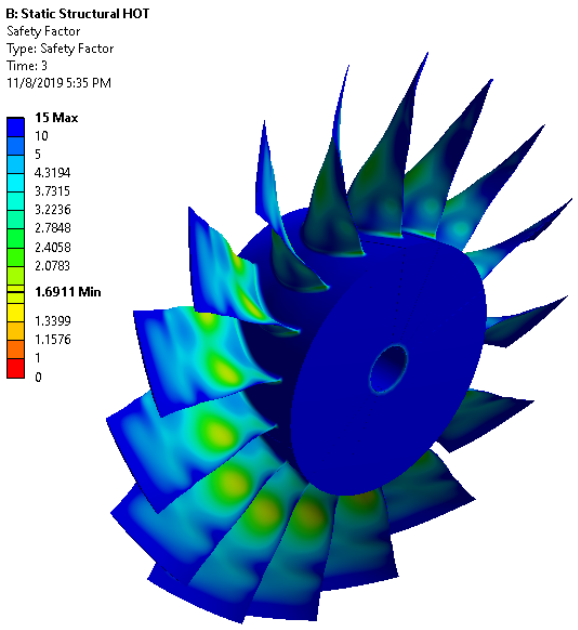

FIGURE 13: YIELD SAFETY FACTOR CONTOUR: $\min f_s = 1.6911$

CONCLUSIONS

This paper discusses a turbomachinery design system which combines a 3D parametric geometry generator, T-Blade3 with the solid modeling system, ESP. The features of this system are illustrated using a single design which used this system with a Genetic Algorithm driven optimization process. T-Blade3 parameterization has been detailed along with the integration with ESP which allows the creation of a solid model of the 3D blade and allows the designer to interact with this model. Finally, a structural analysis using centrifugal and pressure loads for the example geometry has been presented. T-Blade3 source code and documentation along with the input files for this case are available at https://github.com/GTSL-UC/T-Blade3.git. ESP source code or pre-built binaries and documentation are available at https://acdl.mit.edu/ESP.

The authors are continuing work on this design system. Future work involves generalizing the flends obtained from ESP and coupling this design system with a gradient based optimization process geared towards turbomachinery design and optimization.

ACKNOWLEDGEMENTS

This work was partially supported by NASA Glenn Research Center via Vantage Partners, LLC under grant GESS3 GL/TL W141. The first author would like to thank Dr. Kiran Siddappaji for his help with modifying T-Blade3.

REFERENCES

[1] Korikianitis, T., 1993. "Prescribed-Curvature-Distribution Airfoils for the Preliminary Geometric Design of Axial-Turbomachinery Cascades". *Journal of Turbomachinery,* ***115***(2), April, pp. 325–333.

[2] Kulfan, B. M., 2008. "Universal Parametric Geometry Representation Method". *Journal of Aircraft,* ***45***(1), January-February, pp. 142–158.

[3] Gräsel, J., Keskin, A., Swoboda, M., Przewozny, H., and Saxer, A., 2004. "A Full Parametric Model for Turbomachinery Blade Design and Optimisation". In Proceedings of DETC'04, ASME. DETC2004-57467.

[4] Dutta, A. K., Flassig, P. M., and Bestle, D., 2008. "A Non-Dimensional Quasi-3D Blade Design Approach With Respect to Aerodynamic Criteria". In Proceedings of ASME Turbo Expo 2008: Power for Land, Sea and Air, ASME. GT2008-50687.

[5] Koini, G. N., Sarakinos, S. S., and Nikolos, I. K., 2009. "A Software Tool for Parametric Design of Turbomachinery Blades". *Advances in Engineering Software,* ***40***(1), January, pp. 41–51.

[6] Miller, P. L., Oliver, J. H., Miller, D. P., and Tweedt, D. L., 1996. "BladeCAD: An Interactive Geometric Design Tool for Turbomachinery Blades". In 41st Gas Turbine and Aeroengine Congress, ASME.

[7] ANSYS, 2019. https://www.ansys.com/designmodeler.

[8] Siddappaji, K., Turner, M. G., and Merchant, A., 2012. "General Capability of Parametric 3D Blade Design Tool for Turbomachinery". In Proceedings of ASME Turbo Expo 2012: Turbine Technical Conference and Exposition, Vol. 8: Turbomachinery, ASME, pp. 2331–2344. GT2012-69756.

[9] Nemnem, A. F., Turner, M. G., Siddappaji, K., and Galbraith, M., 2014. "A Smooth Curvature-Defined Meanline Section Option for a General Turbomachinery Geometry Generator". In Proceedings of ASME Turbo Expo 2014:

Turbine Technical Conference and Exposition, Vol. 2B: Turbomachinery, ASME, pp. 1–20. GT2014-26363.

[10] Turner, M. G., 2017. "The Role of Curvature in Turbomachinery Design". In Proceedings of the 1st Global Power and Propulsion Forum, Vol. 142, GPPS. GPPF-2017-142.

[11] Balasubramanian, K., Turner, M. G., and Siddappaji, K., 2017. "Novel Curvature-Based Airfoil Parameterization for Wind Turbine Application and Optimization". In Proceedings of ASME Turbo Expo 2017: Turbomachinery Technical Conference and Exposition, Vol. 9: Oil and Gas Applications; Supercritical CO2 Power Cycles; Wind Energy, ASME, pp. 1–11. GT2017-65153.

[12] Mandal, P., 2019. "Design and Optimization of Boundary Layer Ingesting Propulsor". Master's thesis, University of Cincinnati.

[13] Sandia National Laboratory, 2020. DAKOTA. https://dakota.sandia.gov.

[14] Sieradzki, A., Kwiatkowski, T., Turner, M., and Lukasik, B., 2020. "Numerical Modelling and Design Challenges of Boundary Layer Ingesting Fans". In ASME Turbo Expo, ASME. GT2020-15374.

[15] Ugolotti, M., Turner, M., and Orkwis, P., 2019. "An Adjoint-based Sensitivity Formulation Using the Discontinuous Galerkin Method". In AIAA Aviation 2019 Forum, AIAA. 6.2019-3202.

[16] Viars, T., 2020. Optimization of the Design of a Turbine Blade using OpenMDAO. Minithesis, University of Cincinnati. Unpublished.

[17] Youngren, H., and Drela, M., 1991. "Viscous/Inviscid Method for Preliminary Design of Transonic Cascades". In AIAA/SAE/ASME/ASEE 27th Joint Propulsion Conference. 6.1991-2364.

[18] Gray, J. S., Hwang, J. T., Martins, J. R. R. A., Moore, K. T., and Naylor, B. A., 2019. "OpenMDAO:an open-source framework for mutlidisciplinary design, analysis and optimization". *Structural and Multidisciplinary Optimization,* ***59***(4), April.

[19] Haimes, R., and Dannenhoffer, J. F., 2013. "The Engineering Sketch Pad: A Solid-Modeling, Feature-Based, Web-Enabled System for Building Parametric Geometry". In 21st AIAA Computational Fluid Dynamics Conference, AIAA. 6.2013-3073.

[20] Turner, M. G., Merchant, A., and Bruna, D., 2011. "A Turbomachinery Design Tool for Teaching Design Concepts for Axial-Flow Fans, Compressors and Turbines". *Journal of Turbomachinery,* ***133***(3), July.

[21] Wennerstrom, A. J., 2000. *Design of Highly Loaded Axial-Flow Fans and Compressors*. Concepts Eti, Vermont.

[22] Abbott, I. H., and von Doenhoff, A. E., 1949; 1959. *Theory of Wing Sections - Including a Summary of Airfoil Data*. Dover Publications.

[23] Sharma, M., and Turner, M. G., 2020. Application of a Continuous Modified NACA Four Digit Thickness Distribution to Turbomachinery Geometries. To be published in the AIAA Journal.

[24] Mahmood, S. M. H., Turner, M. G., and Siddappaji, K., 2016. "Flow Characteristics of an Optimized Axial Compressor Rotor Using Smooth Design Parameters". In Proceedings of ASME Turbo Expo 2016: Turbomachinery Technical Conference and Exposition, Vol. 2C: Turbomachinery, ASME, pp. 1–12. GT2016-57028.

[25] Waguespack, C., 2014. *Mastering Autodesk Inventor 2015 and Autodesk Inventor LT 2015*. John Wiley & Sons.

[26] Dannenhoffer, J. F., and Haimes, R., 2016. "Generation of Multi-fidelity, Multi-discipline Air Vehicle Models with the Engineering Sketch Pad". In 54th AIAA Aerospace Sciences Meeting, AIAA. 6.2016-1925.

[27] Dannenhoffer, J. F., and Haimes, R., 2017. "Using Design-Parameter Sensitivitites in Adjoint-Based Design Environments". In 55th AIAA Aerospace Sciences Meeting, AIAA. 6.2017-0139.

[28] Canfield, R. A., Alnaqbi, S., Durscher, R. J., Bryson, D. E., and Kolonay, R. M., 2019. "Shape Continuum Sensitivity Analysis using ASTROS and CAPS". In AIAA Scitech 2019 Forum, AIAA. 6.2019-2228.

[29] Meckstroth, C. M., 2019. "Parameterized, Multi-fidelity Aircraft Geometry and Analysis for MDAO Studies using CAPS". In AIAA Scitech 2019 Forum, AIAA. 6.2019-2230.

[30] Karman, S., and Wyman, N., 2019. "Automatic Unstructured Mesh Generation with Geometry Attribution". In AIAA Scitech 2019 Forum, AIAA. 6.2019-1721.

[31] Dannenhoffer, J. F., 2013. "OpenCSM: An Open-Source Constructive Solid Modeler for MDAO". In 51st Aerospace Sciences Meeting, AIAA. 6.2013-0701.

[32] Haimes, R., and Drela, M., 2012. "On The Construction of Aircraft Conceptual Geometry for High-Fidelity Analysis and Design". In 50th AIAA Aerospace Sciences Meeting, AIAA. 6.2012-0683.

[33] OpenCASCADE, 2019. https://www.opencascade.com.

[34] Dannenhoffer, J. F., and Haimes, R., 2015. "Design Sensitivity Calculations Directly on CAD-Based Geometry". In 53rd AIAA Aerospace Sciences Meeting, AIAA. 6.2015-1370.

[35] Holder, J., Turner, M. G., and Celestina, M., 2020. "Automated Turbomachinery Hot-to-Cold Transformation". In AIAA Scitech 2020 Forum, AIAA. 6.2020-0871.

[36] Eager, Z. D., and Dannenhoffer, J. F., 2019. "Flends: Generalized Fillets via B-Splines". In 57th AIAA Aerospace Sciences Meeting, AIAA. 6.2019-1717.

[37] Aerospace Specification Metals, Inc., 2019. Ti-6Al-4V. http://asm.matweb.com/Ti-6Al-4V.